SCIENCE CHINA
Chemistry

• ARTICLES •
• SPECIAL ISSUE • Ionic Liquid and Green Chemistry

August 2012 Vol.55 No.8: 1598–1607
doi: 10.1007/s11426-012-4677-8

Conversion coatings of Mg-alloy AZ91D using trihexyl(tetradecyl) phosphonium bis(trifluoromethanesulfonyl)amide ionic liquid

HOWLETT P. C.[1], GRAMET S.[1], LIN J.[1], EFTHIMIADIS J.[1], CHEN X. B.[2], BIRBILIS N.[2] & FORSYTH M.[1*]

[1]*ARC Centre of Excellence for Electromaterials Science, Institute for Frontier Materials, Deakin University, Burwood Campus, Burwood, Victoria, 3125, Australia*
[2]*CAST Cooperative Research Centre, Department of Materials Engineering, Monash University Melbourne, Victoria, 3800, Australia*

Received April 3, 2012; accepted May 10, 2012; published online July 13, 2012

This work reveals the performance of a trihexyl(tetradecyl)phosphonium bis(trifluoromethanesulfonyl)amide ($[P_{6,6,6,14}][NTf_2]$) ionic liquid (IL) conversion coating upon AZ91D. Such conversion coatings represent a novel avenue for chromate replacement. An optimization of coating performance was pursued by careful alloy pretreatment to generate a surface on which the coating performs best, as the AZ91 substrate is distinctly different from pure or dilute Mg alloys. The results reveal that a functional conversion coating can be achieved, retarding anodic dissolution kinetics, causing a significant decrease in corrosion rate. The coating efficacy is closely tied to the pretreatment performed, which dictates both the microstructural and electrochemical heterogeneity of the surface. The resulting coatings were found to contain Mg_xF_x and phosphonium cation related components, the proportions of which were dependent on the pretreatment.

AZ91D, corrosion, conversion coating, ionic liquid, pretreatment

1 Introduction

Whereas most engineering alloys are resistant to corrosion in moist air due to a protective surface oxide, reactive metals such as magnesium (Mg) possess a surface film whose properties are unable to provide sufficient protection for the underlying metal [1, 2]. Due to this, Mg and its alloys will continue to react with the atmosphere unless an external treatment (e.g., coating or cladding) is used to create a protective barrier [3, 4]. The case for continued efforts to implement Mg into engineered components is clear, with the low density of Mg offering significant light-weighting opportunities that will lead to energy and emissions savings in the transportation industries [5].

Since 1960s [6], protection of Mg from corrosion has been explored using a variety of approaches and chemicals [7, 8]. As for existing technology, anodizing of Mg is technologically challenging (requiring high voltage), and the electroplating of Mg is also hazardous and can be expensive (owing to harsh chemicals used in the process including chromic and hydrofluoric acid). As a result, relatively simple to administer conversion coatings is an industrially attractive method of protection. Conversion coatings for Mg are in most cases comprised of chromates, phosphates, metal oxides or other chemicals that are chemically bonded to the surface [5, 9].

Whilst effective, chromate-based conversion coatings are highly toxic and hence not suitable for mass-market applications. Alternative coatings have been recently developed using stannate [10–12], phosphate [13], permanganate [14], phosphate-permanganate [15–18] and rare earth [19–22] based chemistries. Such conversion coatings, whilst representing various levels of effectiveness, can be satisfactorily

*Corresponding author (email: maria.forsyth@deakin.edu.au)

© Science China Press and Springer-Verlag Berlin Heidelberg 2012

used in many of the less demanding applications for Mg alloys. For the most demanding applications such as transportation, however, suitable chromate replacement coatings still require development and provide the impetus for the work herein.

In recent years, the application of ionic liquids (ILs) in the field of metal surface modification has become of interest [23–25]. ILs have been proposed to be useful in many applications owing to their unique properties, including high thermal and electrochemical stability, low vapor pressure and good ionic conductivity [26, 27].

In recent studies IL baths have been used for electrodeposition of a variety of "difficult" to plate metals upon metal alloys [28]. In such cases the nonaqueous (IL) bath allows the realization of highly negative potentials (since in electrodeposition the metal being coated is the cathode) which results in satisfactory porosity-free coatings with good adhesion. Whilst the use of ILs in electrodeposition will be one of significant promise and future work, in an entirely separate strategy for corrosion protection we have studied the possibility of using ILs to generate conversion coatings upon Mg and its alloys [5, 29–31] and shown that the corrosion properties of metal samples can be improved via the formation of a thin film (~10–100 nm) on the surface of the metal due to immersion in ionic liquids [29].

In a conversion coating the substrate is required to react chemically in the coating electrolyte and therefore the anodic behaviour and the reactivity of the substrate in a given environment takes a critical role. The use of ILs opens a range of specific chemistries to which the substrate may be exposed thereby allowing one to tailor the conversion coating that may form. The work to date has shown that one of the most effective ILs to potentially serve as a conversion coating is that based on trihexyl(tetradecyl)phosphonium bis(trifluoromethanesulfonyl)amide ($[P_{6,6,6,14}][NTf_2]$, Figure 1) [5].

In order to begin to explore this IL conversion coating for Mg in significantly more detail, applicability to commercial and solute rich alloys such as AZ91D is important. In this work the conversion coating of AZ91D in $[P_{6,6,6,14}][NTf_2]$ is studied. The presence of various solute elements such as aluminium and zinc can result in a highly heterogeneous microstructure which of course often leads to a more electrochemically reactive surface, but also may complicate the formation of conversion films. For example in recent work on the commercial alloy ZE41 it was shown that the IL treatments led to highly non-uniform surface films which were less than optimally protective [31]. The differences in reactivity of the various phases was suggested to be the key to the observed film deposition behavior and methods to "homogenise" the activity of the surface such as by applying a potential bias were shown to be promising. In commercial conversion coating technologies the surface of an alloy is normally pretreated prior to coating. The pretreatment can involve anything from wiping, detergent rinsing, grit-blasting, abrading, and exposure to chemicals for functionality, or even cleaning such as degreasing and desmutting. Certainly in the case of aluminum alloys chemical cleaning and pretreatment is standard before conversion coating. Similarly for commercial Mg alloys an appropriate pretreatment to assist in optimization of the subsequent conversion coating is also warranted. In this work we have investigated the influence of pretreating the AZ91 alloy with a protocol designed to homogenise the surface with respect to composition on the $[P_{6,6,6,14}][NTf_2]$ IL generated coatings. Following immersion of the treated and untreated surfaces the corrosion response of AZ91D in Cl^- containing solution was investigated. What is unique about the pretreatment of Mg alloys is that this can be a means of altering, even customizing, the surface chemistry and morphology as a precursor to coating.

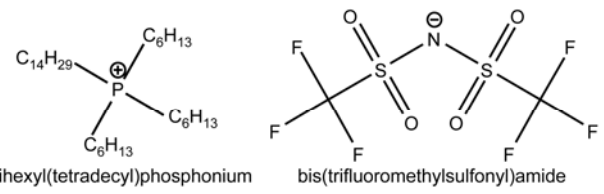

Figure 1 Chemical structure of the ionic liquid $[P_{6,6,6,14}][NTf_2]$.

2 Materials and method

2.1 Materials and pretreatment

The material used in this work was high pressure die cast Mg alloy AZ91D (9 wt% Al, 1 wt% Zn, Balance Mg) with low Fe-impurity content (~40 ppm). Specimens were prepared by grinding with successive grades of SiC paper (320, 600, 1200 grit) and were cleaned with distilled water and ethyl alcohol in an ultrasonic bath. Two pre-treatment procedures, termed the activating (A), and conditioning (C) steps, were applied on AZ91D coupons. A-AZ91D and C-AZ91D represent the specimens which were pre-treated by immersion in a dilute (20 g/L) acidic HNO_3 activating solution (~pH 3) and a concentrated (100 g/L) Na(OH) conditioning solution (~pH 13). The specimens that were pre-treated in activating solution and then in conditioning solution are denoted as A+C-AZ91D.

2.2 Ionic liquid and conversion coating

The IL, $[P_{6,6,6,14}][NTf_2]$ (purchased from Cytec Canada Inc.), contained a 0.1 wt% acid impurity, the presence of which was found to provide improved coating performance. The role of acid content and type is the subject of an ongoing study and will be reported in a future publication. IL conversion coating treatments on both pretreated and unpretreated samples were performed by immersing the AZ91D coupons in $[P_{6,6,6,14}][NTf_2]$ for 24 hours, open to the atmos-

phere at room temperature. The depth of IL above the surface was ~2 mm.

2.3 Electrochemical and exposure testing

In order to measure the conversion coating formation and kinetics in the absence of an electrolyte, electrochemical impedance spectroscopy (EIS) was collected via a pipette-cell [31, 32]. The cell was designed in house in order to allow a portion of a metal surface to be exposed to a relatively small volume of IL and allow coating formation to be studied *in-situ* during the conversion coating stage. The *in-situ* measurements simulate the other treatment processes used to prepare samples for testing, with the exception that the depth of IL is greater (5–10 mm *cf.* 2 mm) above the surface. The clamping of a pipette to the surface defines the working electrode area as the area of the open pipette tip. The counter and the reference electrode were, respectively, a platinum mesh and a platinum wire positioned close to the surface of the coupon. EIS spectra were acquired automatically at 15 minutes intervals over a frequency range from 50 kHz to 10 mHz using 10 mV AC amplitude.

Once conversion coated, cyclic potentiodynamic polarization (CPP) scans were obtained using a conventional three-electrode cell. These tests were performed in 0.01 M NaCl solution (pH 6) using epoxy mounted samples with 1 cm^2 surface area in order to assess the performance of the conversion coatings in a corrosive electrolyte. The counter electrode was a Ti mesh and the reference was a saturated calomel electrode. CPP measurements were acquired after 30 minutes at open circuit potential (OCP) using a Bio-logic VMP 2/Z.

Immersion tests were also done on larger coupons open to the atmosphere at room temperature for 24 hours in 0.01 M NaCl (pH 6). Micrographs were acquired using an optical stereo microscope (Leica MZ6).

2.4 Surface characterisation

Samples for the Australian Synchrotron X-ray photoelectron spectroscopy (XPS) experiments were prepared slightly differently. The 25 mm^2 untreated square shaped coupons were prepared by polishing with SiC paper (600, 1200 and 1200/4000 grit); between each polishing the surface was rinsed with distilled water. All the coupons (untreated and treated) were then rinsed thoroughly with distilled water and absolute ethanol. They were then immersed in absolute ethanol and sonicated for 5 minutes before being dried under nitrogen and stored in the dessicator for 24 hours. Subsequent IL treatments on pretreated and unpretreated samples were performed as above.

The Australian Synchrotron soft X-ray beamline uses an elliptically polarized undulator for the source and is capable of an energy range of 90–2500 eV; details of the design and performance of the beamline are available [33]. The end station is equipped with a SPECS Phoibos 150 Hemispherical Analyser running SpecsLab 2.32-r11458 software (SPECS GmbH). The photon energies were calibrated using the Au $4f_{7/2}$ photoelectron line recorded on a gold disc contained on the sample holder. The X-ray beam to analyzer angle is 55°. The sample is 45° to the X-ray beam (and 80° to the analyzer, i.e. 10° off normal). Dwell time for data acquisition was 0.2 s. The photon flux at the sample ranged from 5×10^{11} to 3×10^{11} photons s^{-1} (storage ring current 200 mA) and the nominal beam size at the sample was 0.15 mm (H)×0.015 mm (V). The photon flux was measured by briefly inserting a GaAs photodiode after the vertical exit slits prior to analysis. Fixed analyser transmission mode was used in medium area mode, with a pass energy of 10 eV for incident photon energy of 790 eV. 10 scans were acquired at 0.1 eV step size. Survey spectra were calibrated to the C1s photoelectron line at 285.0 eV.

The microstructures of AZ91D specimens were investigated via scanning electron microscopy (SEM) using an FEIPhenom SEM. Surface roughness was characterized using a VeecoWyko NT1100 non-contact Optical Profilometer (OP). The EDXS spectra were acquired using the INCA X-Sight 6650, Oxford Instruments, on a Jeol 840 A Tungsten filament SEM with an accelerating voltage of 15 kV, a working distance of 10 mm, and a collection time of 120 s.

3 Results and discussion

3.1 Corrosion performance of IL treated AZ91

Figure 2 shows the effect of exposure of AZ91D substrates to a 0.01 M NaCl solution for 24 hours. Figure 2(a) presents low magnification optical images of as cast AZ91D alloy without any treatment whereas Figures 2(b) and (c) show the effect of the A+C pretreatment alone and A+C pretreatment followed by IL conversion treatment, respectively. From a purely visual perspective a large improvement in corrosion protection is evident for the AZ91 surface following the A+C pretreatment and an even greater improvement when the IL conversion coating is also present.

Figure 3 quantifies these observations by the determination of the number and depths of pits on these surfaces, determined using optical profilometry. The effects of both the A+C pretreatment and subsequent IL treatment are readily seen here with a dramatic decrease in the pitting initiation in both cases but in particular following the IL coating (i.e., an alteration from ~65 pits/mm^2 of 10 μm depth in the as-received AZ91D, compared to ~2 pits/mm^2 following A+C and A+C/IL treatments).

Whilst the A+C treatment significantly reduces the number of larger pits, the subsequent IL conversion coating does not stifle these deeper pits which possibly reflects that the coating is still not perfectly continuous. Any weak spots in the coating when penetrated, will still lead to strong an-

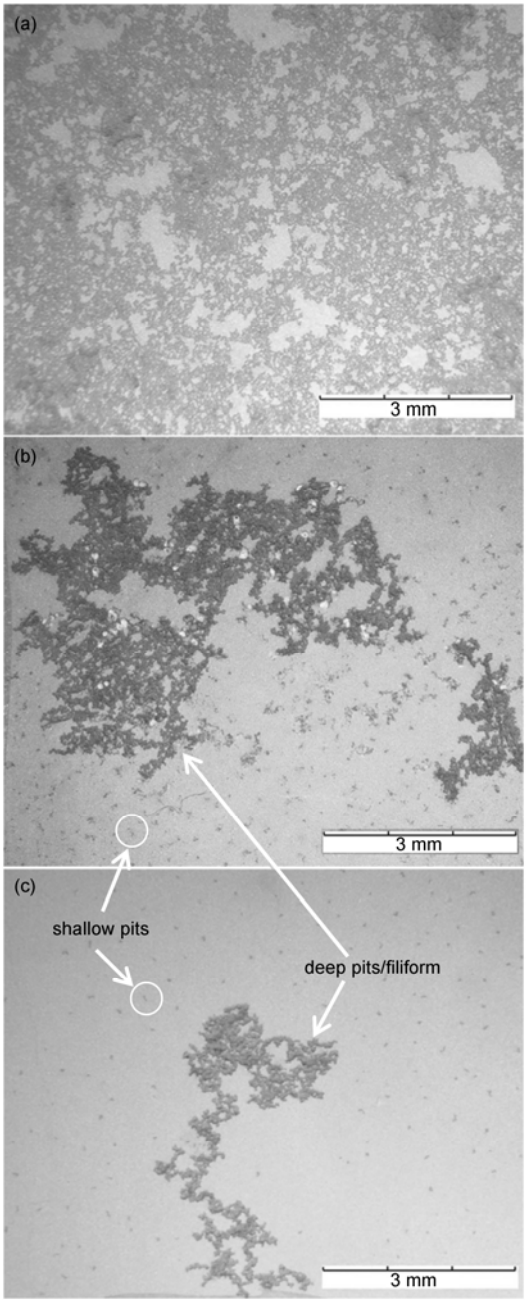

Figure 2 Immersion test images for (a) AZ91D untreated, (b) A+C treated and (c) A+C/24 h IL treated surfaces. The specimens were immersed in 0.01 M NaCl solutions for 24 hours.

odic sites during long term immersion testing. The progression of the defects to deeper pits also suggests that the cathodic reaction is not as significantly affected by the IL treatments as the anodic reaction, an observation supported by the electrochemical data presented in Figure 4.

The improved corrosion performance, and its origins, are further apparent from the electrochemical measurements (Figure 4(a)). Potentiodynamic polarization measurements for the as cast AZ91D, AZ91D + 24 h IL, A+C pretreatment and A+C/IL coating indicate significant differences between

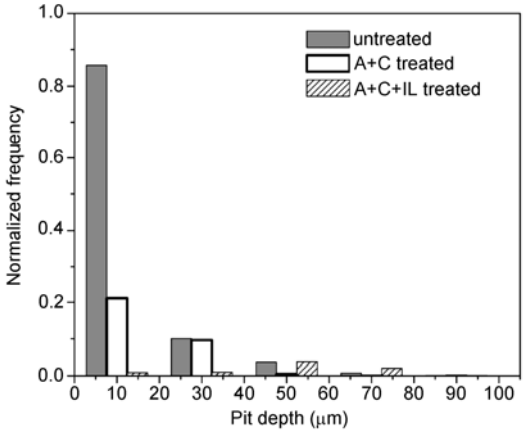

Figure 3 The relative distribution of pit depths for the three surfaces presented in Figure 2.

the untreated surface compared to all other surfaces. The IL treatment alone on the AZ91D provides a significant ennoblement of the surface as previously reported for the AZ31 surface under similar conditions [5]. On the other hand the A+C pretreatments of the AZ91D surface also shift the corrosion potential and the pitting potential to more positive values (−1.3 V compared with −1.47 V versus SCE). However, very promisingly, the combination of A+C and the IL coating further shifts the potential to more noble values as well as significantly reducing the corrosion current by almost an order of magnitude. The trend in the decreasing corrosion current with increasing potential is typified in Figure 4(b). This relationship reveals that the corrosion protection is from anodic control whereby the IL coating stifles anodic reactions but has little impact on the cathodic reaction (the latter of which is dependent on electron transfer and hence suggesting that the thin IL film either does not adequately coat the cathodic β-phase ($Mg_{17}Al_{12}$) or is so thin that it allows for electron transport).

Thus, both the 24 hour immersion testing (as a proxy to long term tests) and the more instantaneous polarization tests (which can give mechanistic insight) indicate that the IL conversion coating is able to provide improved corrosion resistance to the AZ91D alloy and that the combination of A+C pretreatment and IL coating leads to an even higher corrosion resistance. The following discussion attempts to understand the nature of the AZ91D surfaces and the effects of pretreatment and IL coatings on these surfaces.

3.2 Pretreatment and surface modification

The typical surface microstructures following the grinding and pretreatments studied herein are seen in Figure 5. The surface features evident in the four images are distinctly different. For the as-polished AZ91D we observe the typical surface microstructure of this alloy that principally consists of the α-Mg matrix (a Mg-based solid solution containing dissolved Al and Zn) and the β-phase ($Mg_{17}Al_{12}$) interme-

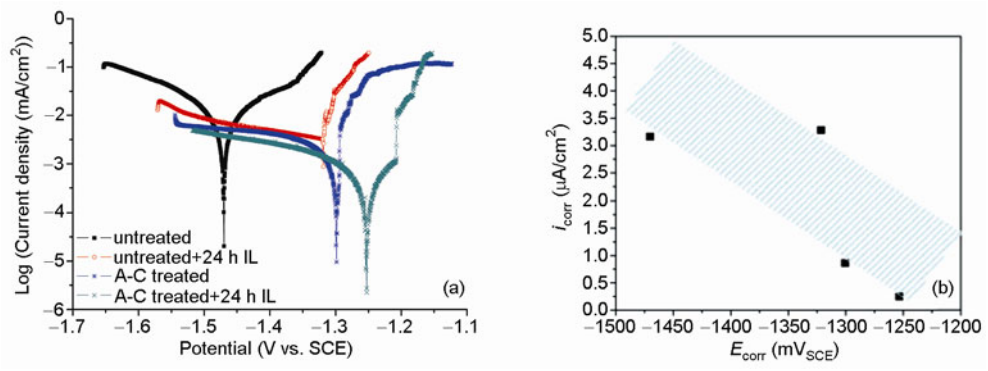

Figure 4 (a) Potentiodynamic polarization curves of AZ91D subject to various pretreatments in 0.01 M NaCl; (b) E_{corr} vs. i_{corr} relationship from (a).

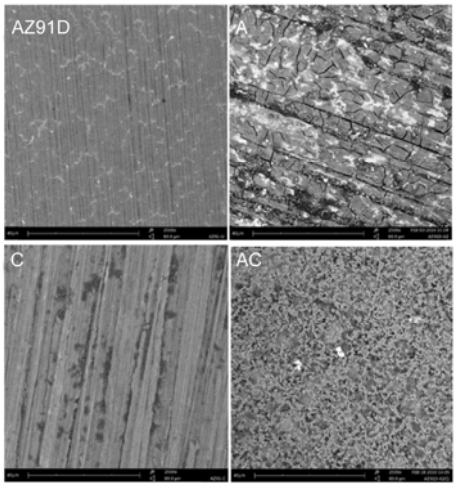

Figure 5 Backscattered SEM images of the magnesium surfaces: (top left) untreated AZ91D, (top right) activator pretreated AZ91D, (bottom left) conditioner pretreated AZ91D, (bottom right) activator + conditioner pretreated AZ91D.

tallic particles that present as the light/white phase. Such a surface is known to be electrochemically heterogeneous and hence highly active and susceptible to corrosion as shown in both the immersion and polarization tests above.

Following activator treatment (Figure 5, A-viz. acid pretreatment), pitting attack of the α phase is readily seen along with some surface cracks and an apparently rougher surface. There does not seem to be any localization of changes related to the β-phase. On the other hand, following the conditioning treatment (Figure 5, C-viz. alkaline pretreatment), the morphology of the α-phase remains essentially unaltered, however we see that the β-phase has been effectively removed from the surface of the alloy. This phenomenon can be explained by the fact that Mg is passive at alkaline pH, whereas Al is very active at such pH values. Finally, the combined A+C treatment produces a surface that has both a high roughness and the absence of β-phase. It is important to note that what we observe following these pretreatments is not the presence of new surface layers but rather a selective modification and dissolution of the AZ91D surface.

The surface roughness (given as the R_a) and surface percentage of Al obtained from these images are summarized in Figure 6. The surface roughness was determined via OP analysis and the wt% Al at the surface was determined from EDXS analysis—thus the data is not point or site specific but represents a general surface value. This data reveals that the as-polished (untreated) AZ91D has a low surface roughness, reflecting the polished surface, and a total surface Al content of between 8 and 9 wt%, which relates to the nominal alloy composition. Following activator treatment (A) the acidic solution attacks the α-Mg matrix thereby increasing roughness and causing an apparent increase in the surface Al content (presumably from incongruent dissolution of the α-Mg matrix which leaves Al remnants from

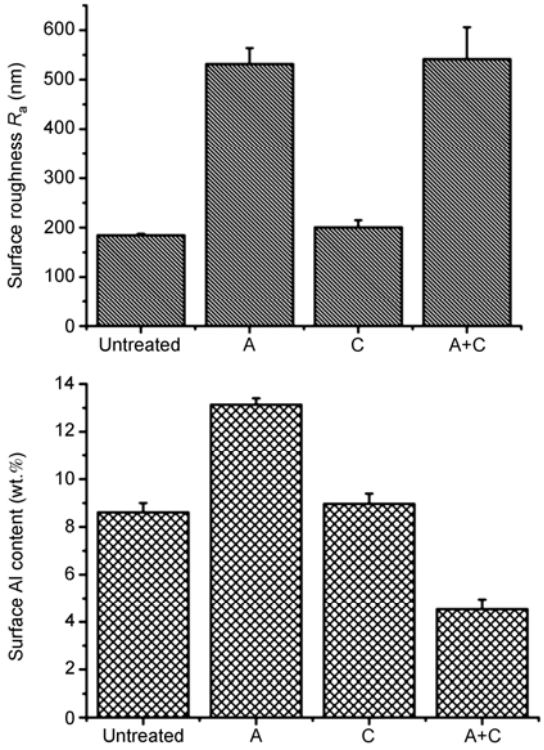

Figure 6 Surface roughness and EDXS determined wt% Al on each of the AZ91D surfaces.

the solid solution to remain on the surface or to redeposit). Conditioner treatment (C) has little effect on the surface roughness, only causing a slight increase in the roughness from where β-phase has been removed. Surprisingly, the surface Al content following Conditioning treatment was almost unchanged and was within the error band of the untreated specimen. This observation is likely owing to the fact that the surface Al content is a combination of the α+β, and that the conditioner treatment may not remove all of the Al from the α phase. We have included the EDXS data as a qualitative descriptor of the role of activator and conditioner, however, the interaction volume of EDXS tests – which can penetrate ~10 μm into the sample–can be of limited quantitative value in such detailed surface analysis and therefore higher resolution surface sensitive XPS (which can also give information on oxides present) was pursued as discussed below.

The A+C treated specimen revealed the highest levels of surface roughness measured which is consistent with the images in Figure 5. The A+C treated specimen also consistently had the lowest value of surface Al content, at times as low as 5 wt% (from a nominal 9% in the alloy composition). This relates well with what is observed for the activator only treated specimen. If the activator treatment causes surface Al to increase by incongruent dissolution of the matrix, then the subsequent conditioner treatment will not only remove β-phase but also the Al species that have been enriched at the surface post-conditioner treatment. Consequently, it can be summarized that following the combined A+C treatment the AZ91D exhibits the most homogenous surface in terms of composition. This is not the case in the Untreated, A or C treated specimens, which still exhibit some chemical inhomogeneity (as is qualitatively evident from Figure 5). This observation can help us understand the corrosion performance of these specimens; the more homogenous surface will likely lead to fewer microgalvanic couples on the AZ91D surface and therefore fewer pits are expected. What is interesting, however, is that the potential of the surface is more noble in the A+C pretreated specimen and one would imagine that a surface richer in Mg may have a more negative, active potential. The reason for this is that it is likely that the final C treatment after the A treatment has also improved the oxide layer on the alloy surface-retarding the anodic kinetics. The polarization data also confirms an Mg-rich surface by the fact that the cathodic kinetics are most sluggish (albeit by only a small amount) compared to all other conditions, consistent with Mg having a much lower exchange current density than Al [34].

3.3 Conversion coating formation

In order to monitor the conversion coating formation process, pipette cell experiments (equivalent to droplet cell experiments [29]) were also executed. The pipette cell experiments expose a small area of alloy to the IL alone (in the absence of a deleterious electrolyte) and allow the conversion coating to be assessed electrochemically via EIS as it is forming.

Figure 7 presents the abridged results of the EIS testing upon AZ91D. Rather than show a large volume of raw electrochemical data, Figure 7 shows a typical variation in the EIS response as judged by the Nyquist plots (inserts). Using a simple Randle's circuit with a constant phase element (Q- which was deemed necessary given the depressed nature of the semi-circles), the capacitance of the surface was determined over a period of 24 h.

A comparison of the initial capacitance value for the as cast AZ91D and the A+C treated specimens immediately illustrates the difference in these two surfaces. The significantly lower capacitance for the A+C treated surface reflects either a thicker oxide film, or a rougher substrate (which may include oxide porosity). Both of these would influence film capacitance in the same way [35], as both can lower rates of metal dissolution, which can also raise surface capacitance. With increasing immersion time in the IL both surfaces display an increase in capacitance although the A+C pretreated surface seems more affected. From a big picture perspective this may suggest that the surface coating is decreasing in thickness, or that surface dissolution reaction rates are being enhanced. The latter is unlikely as we see from the Nyquist plots that charge transfer resistance is increased (total impedance rises) with the IL exposure. Consequently whilst the former may be possible, it is unlikely that dissolution of the native oxide film would lead to an improved corrosion resistance. Instead, we suppose that the IL is able to penetrate the (somewhat porous) oxide film and essentially fill or reduce the size of the pores thereby leading to an apparent increase in capacitance. Ultimately, it is apparent that a film that is more typical of the Mg-IL interaction is replacing the native oxide film. This data also reveals that, as we approach 24 h, the benefits of longer immersion time diminish, with capacitance attaining a maximum at ~3.5 and 1.5 $\mu F/cm^2$, for AZ91D untreated and A+C pretreated surfaces respectively. The duration of these experiments and the rate of coating development may have been affected by the depth of IL above the substrate by limiting the access of atmospheric reactants therefore we note that the time dependence may differ from the bulk experiments.

Some salient points to consider at this stage, are (1) conversion coating times of 24 h are comparatively long when compared to industrial practice which is restricted to a few minutes (in such cases coating thicknesses of many hundreds of nm are achieved rather rapidly); and (2) bearing in mind the prior point, it indicates not only the extent of aqueous electrolyte reactivity but also how non-reactive IL electrolytes can be, thereby revealing very low rates of anodic dissolution of AZ91D over the period of 24 h. Thus the slow reaction between the AZ91D and the IL results in thin films and potentially (in future) the ability to tune the film

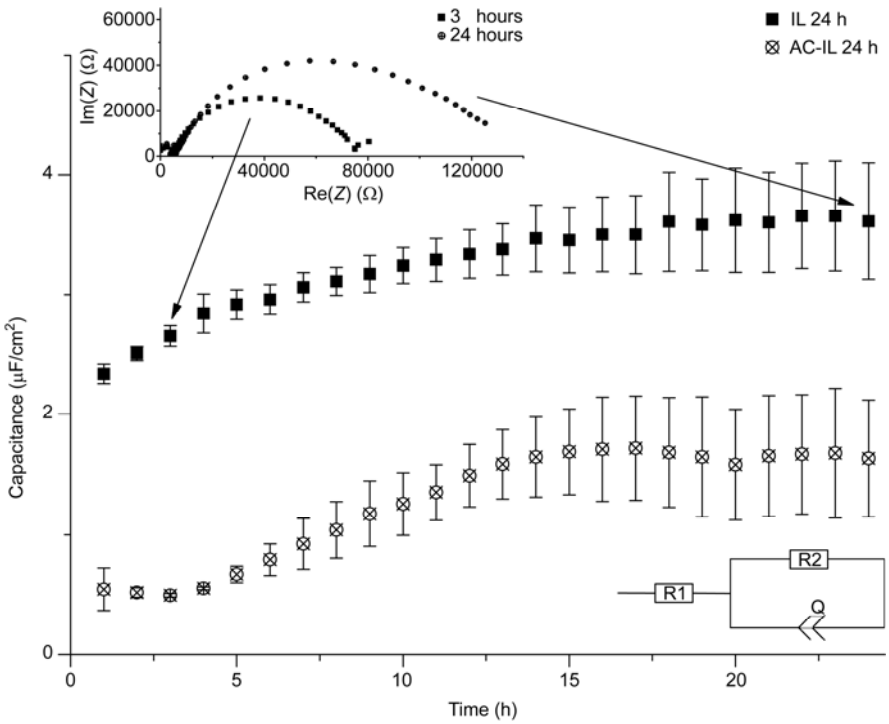

Figure 7 Typical representation of capacitance as a function of immersion time in $[P_{6,6,6,14}][NTf_2]$ IL (i.e., during conversion coating) for AZ91D. Nyquist plots corresponding to ~1 h and ~24 h immersion are inset. Equivalent circuit used is shown. The real capacitance was calculated from the pseudo capacitance according to $C_i = R_i^{(1-n)/n} Y_i^{1/n}$ (where Y is the pseudo capacitance and R is the resistance [38]).

thickness. We have previously shown that the rate of film formation can be increased by the use of moderate temperature (e.g., 50 °C) which reduce treatment times from hours to minutes [5]. In this work, we did not further investigate the affect of time or processing conditions (e.g., temperature) on the coating formation.

3.4 Coated surface characterization

The XPS data presented in Figure 8 and summarized in Table 1 shed some light on the different surfaces formed on the as cast and A+C pretreated specimens when immersed in the IL. On the untreated sample there is evidence of larger quantities of all the ionic liquid components. This is apparent from the F, N, S and P peaks seen in the spectra (Figure 8). Chemically, the surfaces appear very similar (Table 1), with exception of a peak associated with perfluorinated carbons at 292.6 eV on the untreated sample and conversely, a peak indicating the presence of metallic Mg on the A+C IL treated surface. The relative intensities of the IL based peaks appear smaller in the A+C pretreated case and the Mg and Al peaks are also quite prevalent compared with IL only treated AZ91D specimens. In fact, the A+C pretreated and A+C IL treated spectra are very similar, with only very weak IL related peaks present on the IL treated surface. A Photon Energy of 790 eV (*cf.* 1486.6 eV for AlKα) was used in order to obtain more surface sensitive measurements due to poor peak resolution. This suggests a reduced fraction of IL related species on the AZ91 surface, particularly in the A+C pretreated case, compared to previous measurements on AZ31 surfaces [36]. Considering the EIS data (Figure 7) previously discussed (Section 3.3), the occurrence of weaker IL peaks on the A+C IL treated surface supports the notion of the IL penetrating a porous oxide film and the appearance of a relatively large O1s peak on the A+C pretreated and A+C IL treated surfaces agrees with the capacitance and EDXS data which suggest a thicker oxide film. The stronger intensity IL related peaks on the untreated AZ91D surface is consistent with the presence of a film that results in the shift to more noble potentials (compared to untreated and uncoated AZ91D) seen in Figure 4. However, the comparatively small reduction in i_{corr}, suggests a defective or nonuniform film that cannot retard dissolution once pitting commences. In the case of the A+C pretreated specimen a slightly smaller noble shift, relative to the pretreated specimen alone, is observed when the IL coating is also applied. In this case a significantly reduced i_{corr} is observed as well as a further shift of the pitting potential to more positive values, also consistent with a "pore filling" role for the IL generated film.

4 Conclusions

Immersion and polarization testing in NaCl solutions showed that conversion coating in an IL is capable of

Table 1 Binding energies and assignments [36–38] for the relevant photoelectron lines evident on each surface in Figure 8

Photoelectron Line	AZ91D A+C treated	AZ91D 24 h IL treated	AZ91D A+C & 24 h IL treated
F 1s		$-CF_3$ (688.7)	$-CF_3$ (688.6)
F 1s		MgF_2 (685.6)	MgF_2 (685.5)
O 1s	CO_3^{2-}, SO_2^- (531.8)	CO_3^{2-}, SO_2^- (532.3)	CO_3^{2-}, SO_2^- (532.3)
O 1s	$MgO/Mg(OH)_2$ (530.0)		
N 1s		N^- (399.2)	N^- (399.2)
C1s		$-CF_3$ (292.6)	
C 1s	CO_3^{2-} (288.8)	CO_3^{2-} (288.8)	CO_3^{2-} (288.8)
C 1s	C–C/C–H (285.0)	C–C/C–H (285.0)	C–C/C–H (285.0)
C 1s	carbides (below 283.0)		carbides (below 283.0)
S 2p		$-SO_2CF_3$ (169.0)	$-SO_2CF_3$ (169.0)
S 2p		sulfides (below 165.0)	sulfides (below 165.0)
P 2p		alkyl phosphates, P^+ (134.4)	alkyl phosphates, P^+ (134.9)
Al 2p	Al_2O_3 (74.3)	$MgAl_2O_4$, AlF_3 (74.8)	$MgAl_2O_4$, AlF_3 (74.8)
Mg 2p	MgO/MgF_2 (52.0)	MgO/MgF_2 (51.6)	MgO/MgF_2 (51.4)
Mg 2p	$Mg(OH)_2$ (50.4)	$Mg(OH)_2$ (50.4)	$Mg(OH)_2$ (49.9)
Mg 2p	Mg^o (48.3)		Mg^o (48.3)

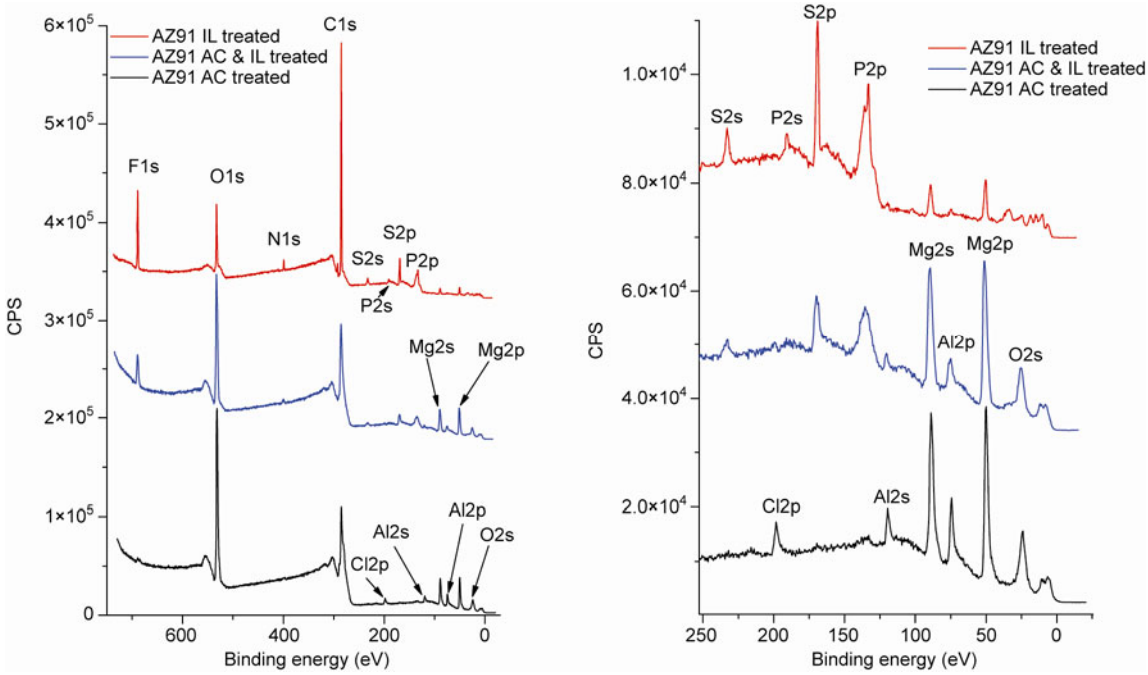

Figure 8 Synchrotron XPS spectra acquired from AZ91D 24 hour IL treated, A+C/24 h IL treated and A+C pretreated surfaces. (a) Survey scan, (b) zoomed section below 250 eV.

providing improved corrosion resistance of Mg-alloy AZ91D. Such a finding gives significant merit to pursuit of conversion coatings from ILs where there is scope (largely unexplored) to tailor the conversion coating bath composition (whilst being water free) to provide functionality. This latter point is important for Mg alloys, since the presence of water in aqueous conversion coating baths leads to rapid surface reaction and potentially undesirable products. We

contend that coating times of 24 h are industrially impractical, however in future work will investigate controlling the reactivity of the IL. This may be through the use of an activator (e.g. water, base or acid) and, as already mentioned, the use of elevated temperature which has been shown to reduce coating formation times [5].

There are many aspects of IL conversion coatings that require significant future work, including and not limited to: understanding which species inside the IL are forming the functional surface, the persistence of the conversion coating on the surface and how long it will last, the corrosion resistance that can be expected from the IL conversion coating and the importance of parameters such as temperature and moisture solubility.

It was seen herein that chemical pretreatment can have a marked effect on both the surface roughness and the surface composition of AZ91D. The development of a chemically homogenous and Mg rich surface prior to conversion coating is beneficial in the development of optimized IL coatings. The most homogenous coating was shown to be the A+C treatment, which had the highest surface activity. The IL coatings were shown to be effective at dramatically retarding the rate of anodic dissolution of AZ91D. This results in an ennoblement of E_{corr} and a concomitant decrease in i_{corr}. Cathodic kinetics were largely unaffected by the IL coatings studies herein. This suggests that the IL coating does not adequately protect the cathodic β-phase, yet restricts dissolution of Mg from the α-phase.

Based on synchrotron XPS, the nature of the IL film includes native oxides, hydroxides and carbonates which are remnant from the previous surface preparation. In the case of the A+C pretreated surface this constitutes a thicker oxide dominated film in which IL related species (species related to both the cation and anion as well as anion breakdown products [36], are evident) appear to have penetrated and modified the remnant surface film.

We gratefully acknowledge the Australian Research Council for the financial support through DP0986205. The CAST Co-operative Research Centre was established under, and is funded in part by, the Australian Governments Co-operative Research Centres Scheme. This research was undertaken on the Soft X-ray beamline at the Australian Synchrotron, Victoria, Australia. The authors wish to thank Dr Bruce Cowie and Dr Lars Thomsen for their assistance and support during acquisition of the XPS data.

1 Boyer JA. *The Corrosion of Magnesium and of Magnesium Alloys Containing Manganese*. Corporation AM. ed. American Magnesium Corporation, 1927
2 Song G, Atrens A, St John D, Zheng L. *Magnesium Alloys and Their Applications*. WIley-VCH, Vol. 245, 2000
3 Macdonald DD. Passivity—the key to our metals-based civilization. *Pure Appl Chem*, 1999, 71(6): 951–978
4 Evans UR. *An Introduction to Metallic Corrosion,* 3rd ed. London: Edward Arnold, 1981, 302
5 Forsyth M, Howlett PC, Tan SK, Mac Farlane DR, Birbilis N. An ionic liquid surface treatment for corrosion protection of magnesium alloy AZ31. *Electrochem Solid-State Lett*, 2006, 9(11): B52–B55
6 Lorking KF. Inhibition of corrosion of magnesium in chromic acid. *Nature,* 1964, 201(491): 75
7 Hehmann F, Sommer F, Jones H, Edyvean RGJ. Corrosion inhibition in magnesium aluminum-based alloys induced by rapid solidification processing. *J Mater Sci*, 1989, 24(7): 2369–2379
8 Ma Y, Nie X, Northwood DO, Hu H. Systematic study of the electrolytic plasma oxidation process on a mg alloy for corrosion protection. *Thin Solid Films*, 2006, 494(1-2): 296–301
9 Chen XB, Birbilis N, Abbott TB. Review of corrosion-resistant conversion coatings for magnesium and its alloys. *Corrosion*, 2011, 67(3): 035005-1–035005-16
10 Gonzaleznunez MA, Nunezlopez CA, Skeldon P, Thompson GE, Karimzadeh H, Lyon P, Wilks TE. A non-chromate conversion coating for magnesium alloys and magnesium-based metal-matrix composites. *Corros Sci*, 1995, 37(11): 1763–1772
11 Anicai L, Masi R. Santamaria M, Di Quarto F. A photoelectrochemical investigation of conversion coatings on Mg substrates. *Corros Sci*, 2005, 47(12): 2883–2900
12 Lin CS, Lin HC, Lin KM, Lai WC. Formation and properties of stannate conversion coatings on AZ61 magnesium alloys. *Corros Sci*, 2006, 48(1): 93–109
13 Kouisni L, Azzi M, Zertoubi M, Dalard F, Maximovitch S. Phosphate coatings on magnesium alloy AM60 Part 1: Study of the formation and the growth of zinc phosphate films. *Surf Coat Technol*, 2004, 185(1): 58–67
14 Umehara H, Takaya M, Terauchi S. Chrome-free surface treatments for magnesium alloy. *Surf Coat Technol*, 2003, 169: 666–669
15 Chong KZ, Shih TS. Conversion-coating treatment for magnesium alloys by a permanganate-phosphate solution. *Mater Chem Phys*, 2003, 80(1): 191–200
16 Hawke D, Albright DL. A phosphate-permanganate conversion coating for magnesium. *Metal Finishing*, 1995, 93(10): 34–38
17 Lin CS, Lee CY, Li WC, Chen YS, Fang GN. Formation of phosphate/permanganate conversion coating on AZ31 magnesium alloy. *J Electrochem Soc*, 2006, 153(3): B90–B96
18 Zhao M, Wu SS, Luo JR, Fukuda Y, Nakae H. A chromium-free conversion coating of magnesium alloy by a phosphate-permanganate solution. *Surf Coat Technol*, 2006, 200(18-19): 5407–5412
19 Dabala M, Brunelli K, Napolitani E, Magrini M. Cerium-based chemical conversion coating on AZ63 magnesium alloy. *Surf Coat Technol*, 2003, 172(2-3): 227–232
20 Brunelli K, Dabala M, Calliari I, Magrini M. Effect of Hcl pre-treatment on corrosion resistance of cerium-based conversion coatings on magnesium and magnesium alloys. *Corros Sci*, 2005, 47(4): 989–1000
21 Lin CS, Fang SK. Formation of cerium conversion coatings on AZ31 magnesium alloys. *J Electrochem Soc*, 2005, 152(2): B54–B59
22 Rudd AL, Breslin CB, Mansfeld F. The corrosion protection afforded by rare earth conversion coatings applied to magnesium. *Corros Sci*, 2000, 42(2): 275–288
23 Zein El Abedin S, Endres F. Electrodeposition of metals and semiconductors in air- and water-stable ionic liquids. *ChemPhysChem*, 2006, 7(1): 58–61
24 Bermudez MD, Jimanez AE, Martinez-Nicolls G. Study of surface interactions of ionic liquids with aluminium alloys in corrosion and erosion-corrosion processes. *Appl Surf Sci,* 2007, 253(17): 7295–7302
25 Caporali S, Ghezzi F, Giorgetti A, Lavacchi A, Tolstogouzov A, Bardi U. Interaction between an imidazolium based ionic liquid and the az91d magnesium alloy. *Adv Eng Mater,* 2007, 9(3): 185–190
26 Welton T. Room-temperature ionic liquids. solvents for synthesis and catalysis. *Chem Rev*, 1999, 99(8): 2071–2083
27 MacFarlane DR, Forsyth M, Howlett PC, Pringle JM, SunJ, Annat G, Neil W, Izgorodina EI. Ionic liquids in electrochemical devices and processes: Managing interfacial electrochemistry. *Acc Chem Res*, 2007, 40(11): 1165–1173
28 Yang H, Guo X, Wu G, Ding W, Birbilis N. Electrodeposition of chemically and mechanically protective Al-coatings on AZ91DMg alloy. *Corros Sci*, 2011, 53(1): 381–387

29 Birbilis N, Howlett PC, MacFarlane DR, Forsyth M. Exploring corrosion protection of Mg via ionic liquid pretreatment. *Surf Coat Technol*, 2007, 201(8): 4496–4504
30 Howlett PC, Zhang S, MacFarlane DR, Forsyth M. An investigation of a phosphinate-based ionic liquid for corrosion protection of magnesium alloy AZ31. *Aust J Chem*, 2007, 60(1): 43–46
31 Efthimiadis J, Neil WC, Bunter A, Howlett PC, Hinton BRW, MacFarlane DR, Forsyth M. Potentiostatic control of ionic liquid surface film formation on ZE41 magnesium alloy. *ACS App Mater Int*, 2010, 2(5): 1317–1323
32 Howlett PC, Khoo T, Mooketsi G, Efthimiadis J, MacFarlane DR, Forsyth M. The effect of potential bias on the formation of ionic liquid generated surface films on Mg alloys. *Electrochim Acta*, 2010, 55(7): 2377–2383
33 Cowie BCC, Tadich A, Thomsen L. The current performance of the wide range (90–2500 eV) soft X-ray beamline at the australian synchrotron. *AIP Conference Proceedings,* 2010, 1234(1): 307–310
34 Südholz AD, Kirkland NT, Buchheit RG, Birbilis N. Electrochemical properties of intermetallic phases and common impurity elements in magnesium alloys. *Electrochem Solid-State Lett*, 2011, 14(2): C5–C7
35 Wang H, Shi H, Hong T, Kang C, Jepson WP. *Characterization of Inhibitor and Corrosion Product Film Using Electrochemical Impedance Spectroscopy (EIS)*. in NACE International Corrosion Conference and Expo, 2001, NACE: Houston, TX, USA
36 Howlett PC, Efthimiadis J, Hale P, Van Riessen GA, MacFarlane DR, Forsyth M. Characterization of the magnesium alloy AZ31 surface in the ionic liquid trihexyl(tetradecyl)phosphonium bis(trifluoromethanesulfonyl) amide. *J Electrochem Soc*, 2010, 157(11): C392–C398
37 Moulder JF, ChastainJ, StickleWF, Sobol PE, BombenKD. *Handbook of X-Ray Photoelectron Spectroscopy: A Reference Book of Standard Spectra for Identification and Interpretation of XPS Data*. Physical Electronics, 1995
38 Howlett PC, Brack N, Hollenkamp AF, Forsyth M, MacFarlane DR. Characterization of the lithium surface in *N*-methyl-*N*-alkylpyrrolidinium bis(trifluoromethanesulfonyl) amide room-temperature ionic liquid electrolytes. *J Electrochem Soc*, 2006, 153(3): A595–A606